Male Sterile2 Encodes a Plastid-Localized Fatty Acyl Carrier Protein Reductase Required for Pollen Exine Development in Arabidopsis[1[C][W][OA]]

Weiwei Chen[2], Xiao-Hong Yu[2], Kaisi Zhang, Jianxin Shi, Sheron De Oliveira, Lukas Schreiber, John Shanklin, and Dabing Zhang*

Institute of Plant Science, State Key Laboratory of Hybrid Rice, School of Life Sciences and Biotechnology, Shanghai Jiao Tong University, Shanghai 200240, China (W.C., K.Z., J. Shi, D.Z.); Department of Biology, Brookhaven National Laboratory, Upton, New York 11973 (X.-H.Y., J. Shanklin); and Institute of Cellular and Molecular Botany, University of Bonn, D–53115 Bonn, Germany (S.D.O., L.S.)

Male Sterile2 (*MS2*) is predicted to encode a fatty acid reductase required for pollen wall development in Arabidopsis (*Arabidopsis thaliana*). Transient expression of MS2 in tobacco (*Nicotiana benthamiana*) leaves resulted in the accumulation of significant levels of C16 and C18 fatty alcohols. Expression of MS2 fused with green fluorescent protein revealed that an amino-terminal transit peptide targets the MS2 to plastids. The plastidial localization of MS2 is biologically important because genetic complementation of *MS2* in *ms2* homozygous plants was dependent on the presence of its amino-terminal transit peptide or that of the Rubisco small subunit protein amino-terminal transit peptide. In addition, two domains, NAD(P)H-binding domain and sterile domain, conserved in MS2 and its homologs were also shown to be essential for MS2 function in pollen exine development by genetic complementation testing. Direct biochemical analysis revealed that purified recombinant MS2 enzyme is able to convert palmitoyl-Acyl Carrier Protein to the corresponding C16:0 alcohol with NAD(P)H as the preferred electron donor. Using optimized reaction conditions (i.e. at pH 6.0 and 30°C), MS2 exhibits a K_m for 16:0-Acyl Carrier Protein of 23.3 ± 4.0 μM, a V_{max} of 38.3 ± 4.5 nmol mg^{-1} min^{-1}, and a catalytic efficiency/K_m of 1,873 M^{-1} s^{-1}. Based on the high homology of MS2 to other characterized fatty acid reductases, it was surprising that MS2 showed no activity against palmitoyl- or other acyl-coenzyme A; however, this is consistent with its plastidial localization. In summary, genetic and biochemical evidence demonstrate an MS2-mediated conserved plastidial pathway for the production of fatty alcohols that are essential for pollen wall biosynthesis in Arabidopsis.

In flowering plants, the life cycle alternates between diploid sporophyte and haploid gametophyte generations. Pollen grains play a biologically protective role for the haploid male sperm cells surrounded by the outer cell wall lipidic biopolymers called the exine (Blackmore et al., 2007; Li and Zhang, 2010; Ariizumi and Toriyama, 2011). Pollen exine protects the gametophyte against pathogen attack, dehydration, and UV irradiation as well as facilitates the pollination process, including pollen recognition and adhesion to the stigma. The highly durable exine that occurs throughout flowering plants is thought to play an essential role in land colonization by plants (Chaloner, 1976).

The exine is mainly composed of the biopolymer sporopollenin and contains two sublayers, the sexine and nexine (Zinkl et al., 1999). The biochemical nature of pollen exine remains largely unknown because of the technical difficulties in purifying and obtaining large quantities of materials for analysis. In addition, sporopollenin is highly insoluble, resistant to degradation, and exceptionally stable (Brooks and Shaw, 1968; Bubert et al., 2002). Current evidence suggests that the major components of sporopollenin are derivatives of aliphatics, such as fatty acids and phenolic compounds (Bubert et al., 2002; Blackmore et al., 2007).

Tapetum, the innermost sporophytic anther wall layer, is thought to play a major role in actively synthesizing and secreting sporopollenin precursors onto the microspore surface for pollen exine polymerization and patterning (Bedinger, 1992; Li and Zhang, 2010; Ariizumi and Toriyama, 2011). The model dicot plant Arabidopsis (*Arabidopsis thaliana*) and many other plants have a secretory-type tapetum with spe-

[1] This work was supported by the National Basic Research Program of China (grant no. 2009CB941500), the National Natural Science Foundation of China (grant no. 30725022), the Shanghai Leading Academic Discipline Project (grant no. B205), the U.S. Department of Energy Basic Energy Sciences program (to J. Shanklin), and the U.S. National Science Foundation (grant no. DBI 0701919 to X.-H.Y.).

[2] These authors contributed equally to the article.

* Corresponding author; e-mail zhangdb@sjtu.edu.cn.

The author responsible for distribution of materials integral to the findings presented in this article in accordance with the policy described in the Instructions for Authors (www.plantphysiol.org) is: Dabing Zhang (zhangdb@sjtu.edu.cn).

[C] Some figures in this article are displayed in color online but in black and white in the print edition.

[W] The online version of this article contains Web-only data.

[OA] Open Access articles can be viewed online without a subscription.

www.plantphysiol.org/cgi/doi/10.1104/pp.111.181693

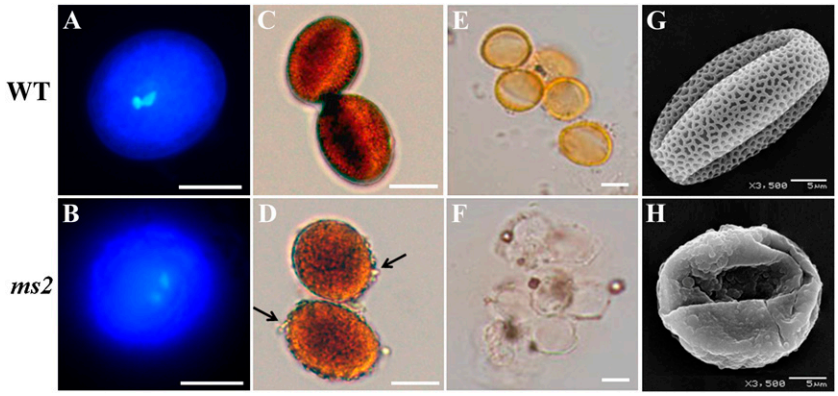

Figure 1. Pollen phenotype of the *ms2* mutant. Pollen grains isolated from a wild-type (WT) plant and a *ms2* plant were detected by DAPI staining (A and B), I_2-KI staining (C and D), acetolysis treatment (E and F), and SEM (G and H). Arrows in D show the rough outer surface of *ms2* pollen grains. Bars = 10 μm (A–F) and 5 μm (G and H).

cialized structures such as tapetosomes in the cells, which accumulate lipidic components (Huysmans et al., 1998). The outer surface of Arabidopsis pollen grains displays elegant reticulate cavities with abundant pollen coat (tryphine) deposited inside the pollen exine.

Pollen exine patterning appears to include at least three major developmental events: callose wall formation, primexine formation, and sporopollenin synthesis (Ariizumi and Toriyama, 2011). Exine formation commences after meiosis, with the accumulation of lipidic precursors onto the primexine surrounding newly formed microspores between the callose wall and the microspore plasma membrane (Paxson-Sowders et al., 2001; Blackmore et al., 2007). After the first pollen mitosis, the synthesis of the exine is almost complete; and during later stages of pollen exine formation, the pectocellulosic intine and the tryphine, called the pollen coat, are deposited onto the pollen wall (Piffanelli et al., 1998). Recent genetic and biochemical investigations showed that some genes, including *MALE STERILITY1* (*MS1*), *MS2*, *CER1*, *NO EXINE FORMATION1*, *FACELESS POLLEN1*, *CYP703A2*, *ACYL-COA SYNTHETASE5* (*ACOS5*), *CYP704B1*, *TETRAKETIDE α-PYRONE REDUCTASE1* and *-2* (*TKPR1/2*), *LAP6/POLYKETIDE SYNTHASE A* (*PKSA*), and *LAP5/POLYKETIDE SYN-*

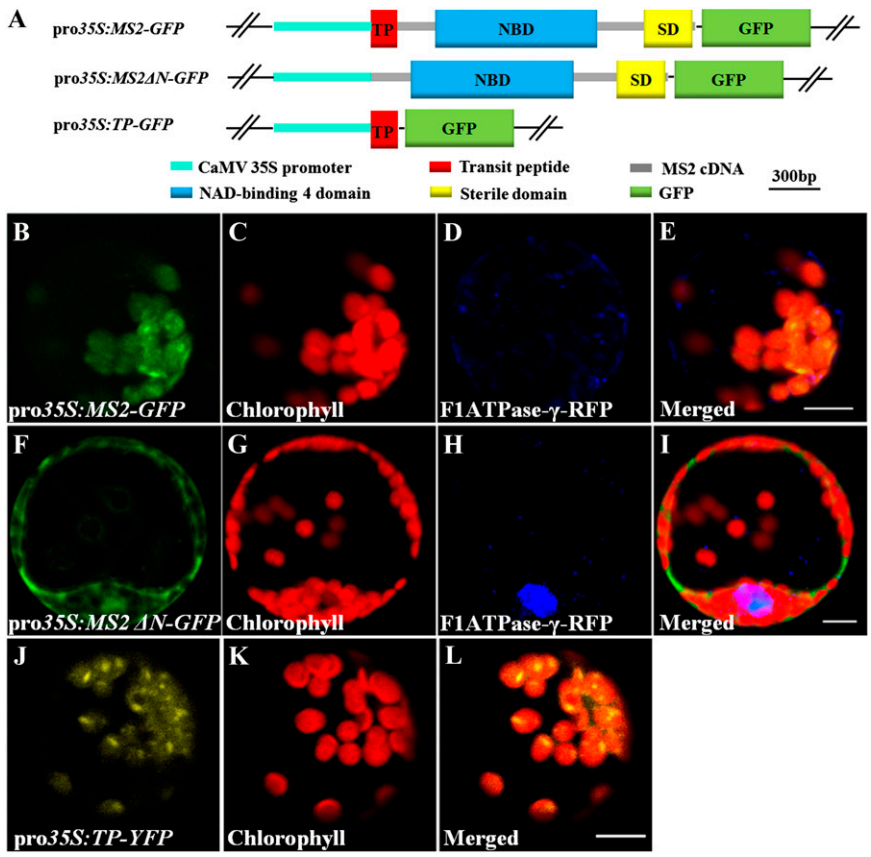

Figure 2. Subcellular localization analysis of MS2 in protoplasts. A, Diagrams of the constructs of the full-length *MS2* cDNA with and without the sequence encoding the putative transit peptide (TP) fused with the N terminus of GFP under the control of the *CaMV 35S* promoter (pro*35S:MS2-GFP* and pro*35S:MS2ΔN-GFP*, respectively) and the fragment encoding the putative transit peptide of MS2 fused with YFP under the control of the *CaMV 35S* promoter (pro*35S:TP-YFP*). B to E, An Arabidopsis protoplast expressing MS2-GFP showing green fluorescent signals (B), the chlorophyll autofluorescence signals in the chloroplasts (C), blue fluorescent signals by coexpressing mitochondrion-localizing F1ATPase-γ-RFP (D), and the merged signals (E). F to I, An Arabidopsis protoplast expressing MS2ΔN-GFP showing green fluorescent signals in the cytoplasm (F), the chlorophyll autofluorescence signals (G), blue fluorescent signals by coexpressing mitochondrion-localizing F1ATPase-γ-RFP (H), and the merged signals (I). J to L, An Arabidopsis protoplast expressing TP-YFP showing yellow fluorescent signals (J), the chlorophyll autofluorescence signals in the plastids (K), and the merged signals (L). Bars = 10 μm.

THASE B (*PKSB*) in Arabidopsis (Aarts et al., 1995, 1997; Wilson et al., 2001; Ariizumi et al., 2003, 2004; Morant et al., 2007; de Azevedo Souza et al., 2009; Dobritsa et al., 2009, 2010; Grienenberger et al., 2010; Kim et al., 2010b) as well as *Tapetum Degeneration Retardation*, *Wax-Deficient Anther1*, *CYP704B2*, *C6*, *Post-meiotic Deficient Anther1*, and *Persistent Tapetal Cell1* in rice (*Oryza sativa*; Jung et al., 2006; Zhang et al., 2008, 2010, 2011; Hu et al., 2010; Li et al., 2006, 2010, 2011; Li and Zhang, 2010), are required for pollen exine synthesis. However, relatively little has been described on the biochemical aspects of these gene products.

Fatty alcohols are widely observed in plants, animals, and algae in free forms (the component of cuticular lipids) but more frequently in esterified (wax esters) or etherified (glyceryl ethers) forms. Fatty alcohols and their derivatives are major components of the lipidic anther cuticle and pollen wall (Ahlers et al., 1999; Kunst and Samuels, 2003; Jung et al., 2006; Li et al., 2010). Previous investigations revealed that fatty acyl-CoAs are thought to be used as substrates for the production of fatty alcohols by fatty acyl-coenzyme A reductase (FAR) in garden pea (*Pisum sativum*), jojoba (*Simmondsia chinensis*), Arabidopsis, wheat (*Triticum aestivum*), mouse (*Mus musculus*), and silk moth (*Bombyx mori*; Aarts et al., 1997; Metz et al., 2000; Wang et al., 2002; Moto et al., 2003; Cheng and Russell, 2004; Rowland et al., 2006; Doan et al., 2009; Domergue et al., 2010).

MS2 was assumed to encode a FAR-like protein that converts fatty acids to alcohols. *MS2* was shown to be expressed in the tapetum shortly after the microspore was released from the tetrad (Aarts et al., 1997). *ms2* mutants display abnormal pollen wall development, which is sensitive to acetolysis treatment, causing reduced pollen fertility (Aarts et al., 1997; Dobritsa et al., 2009). However, detailed biochemical characterization of the MS2 enzyme has not been performed. Recently, recombinant bacteria expressing five Arabidopsis FAR homologs were shown to produce fatty alcohols with carbon lengths of C14, C16, and C18 from endogenous bacterial fatty acids. Bacteria expressing MS2 are able to form C14:0, C16:0, and C18:1 alcohols (Doan et al., 2009). Furthermore, yeast cells expressing FAR1, FAR4, and FAR5 are able to produce alcohols using distinct but overlapping substrates with a chain length ranging from C18:0 to C24:0 (Domergue et al., 2010).

In this study, we report the biochemical characterization of MS2. We show that *MS2* encodes a fatty acyl-Acyl Carrier Protein (ACP) reductase, and the purified recombinant MS2 enzyme from *Escherichia coli* is able to convert the preferred substrate palmitoyl-ACP to C16:0 alcohol in the presence of NAD(P)H. In addition, MS2 possesses an N-terminal transit peptide that is necessary for localization to the plastid. The biological significance of MS2 subcellular localization, and the presence of conserved domains/motifs within MS2, were demonstrated by genetic complementation of *ms2* mutants. This work, therefore, demonstrates the involvement of the plastid in primary fatty alcohol synthesis required for pollen wall development in Arabidopsis.

RESULTS

ms2 Pollen Grains Have Defective Pollen Exine

Defective pollen grains of *ms2* were incubated with 4′,6-diamidino-2-phenylindole (DAPI) and iodine-potassium iodide (I_2-KI). DAPI staining showed that both the wild type and *ms2* display normal mature pollen grains with a single vegetative nucleus and two sperm nuclei at the mature pollen developmental stage (Fig. 1, A and B). I_2-KI staining revealed that *ms2* pollen grains had a rough outer surface compared with the wild type (Fig. 1, C and D), consistent with the defective pollen wall development of *ms2*. In agreement with previous reports (Aarts et al., 1997; Dobritsa et al., 2009), *ms2* pollen grains were sensitive to acetolysis treatment (Fig. 1, E and F), and scanning electron microscopy (SEM) analysis revealed that the *ms2* pollen grains collapsed and attained a severely shrunken appearance (Fig. 1, G and H).

The MS2 Protein Is Localized to Plastids

Previous investigation predicted that MS2 (At3g11980) and a MS2 homolog (At3g56700) were localized in chloroplasts based on the presence of an N-terminal transit peptide (Doan et al., 2009). Our TargetP 1.1, ChloroP 1.1, and MitoProt II version 1.101 sequence analyses consistently suggested that the MS2 protein contained a putative plastid-targeting (or mitochon-

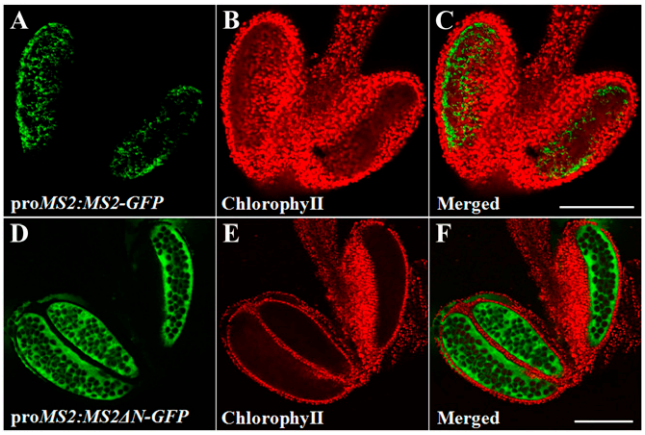

Figure 3. Localization of *MS2* expression in transgenic plants. A to C, A transgenic plant line expressing full-length MS2 cDNA fused with GFP under the control of the *MS2* promoter (pro*MS2*:*MS2-GFP*) in the wild type, showing green fluorescent signals in the tapetal layer (A), autofluorescence signals of chlorophyll (B), and the merged signals (C). D to F, A transgenic plant line expressing *MS2* cDNA without the sequence encoding the putative transit peptide fused with GFP under the control of the *MS2* promoter (pro*MS2*:*MS2ΔN-GFP*) showing green fluorescent signals (D), autofluorescence signals of chlorophyll (E), and the merged signals (F). Bars = 100 μm.

drion-targeting) peptide with 46 amino acid residues at the N terminus. In order to determine the subcellular localization of MS2, we made two constructs, pro*35S*:*MS2-GFP* and pro*35S*:*MS2*△*N-GFP*, driven by the cauliflower mosaic virus (*CaMV*) *35S* promoter. pro*35S*:*MS2-GFP* contained the full-length *MS2* cDNA translationally fused to the 5′ terminus of *GFP*, and in pro*35S*:*MS2*△*N-GFP*, the N-terminal transit peptide portion of the *MS2* cDNA was deleted and the MS2 polypeptide was translationally fused with GFP (Fig. 2A). Chloroplasts were identified by the autofluorescence of chlorophyll, and a translational fusion construct of the mitochondrial F1ATPase γ-subunit with red fluorescent protein (RFP) was used to mark the mitochondrion (Kim et al., 2006). Analysis using Arabidopsis protoplasts from leaf cells showed that the MS2-GFP signal colocalized with the chlorophyll autofluorescence signal in chloroplasts but not obviously with the F1ATPase-γ-RFP signal in Arabidopsis protoplasts (Fig. 2, B–E), consistent with MS2 localization in plastids. In contrast, the MS2△N-GFP signals were observed in the cytoplasm and did not colocalize with the RFP signal or the chlorophyll autofluorescence signal (Fig. 2, F–I). Furthermore, we fused the DNA fragment of the MS2 N-terminal transit peptide to *GFP* and confirmed that the transit peptide of MS2 is able to target the GFP into chloroplasts using pro*35S*:*TP-YFP* (for transit peptide-yellow fluorescent protein; Fig. 2, J–L). In addition, the localization of MS2 in plastids was also confirmed in transgenic tobacco (*Nicotiana benthamiana*) leaves transiently expressing *MS2-GFP*, *MS2*△*N-GFP*, and free *GFP* (Supplemental Fig. S1).

The expression of *MS2* was shown only in tapetal cells at or very shortly after young microspores were released from the tetrad by in situ RNA hybridization and promoter fused with the GUS reporter gene analyses (Aarts et al., 1997). In this study, we observed the GFP signal of pro*MS2-GFP* in the tapetal cells at the free microspore stage in the stable transgenic lines (Fig. 3, A–C). Furthermore, the fluorescent signal in the anthers of transgenic lines harboring pro*MS2*△*N-GFP* showed higher expression signals in tapetal cells and anther locules compared with those of transgenic lines containing pro*M2-GFP* (Fig. 3, D–F), suggesting that the N-terminal transit peptide of MS2 is responsible for correct MS2 localization, the absence of which possibly affects its turnover.

The biological importance of the MS2 localization to plastids was confirmed from the observation that the construct pro*M2*:*MS2*△*N* without the N-terminal transit peptide-encoding sequence of MS2 could not complement the defective pollen wall development in *ms2*

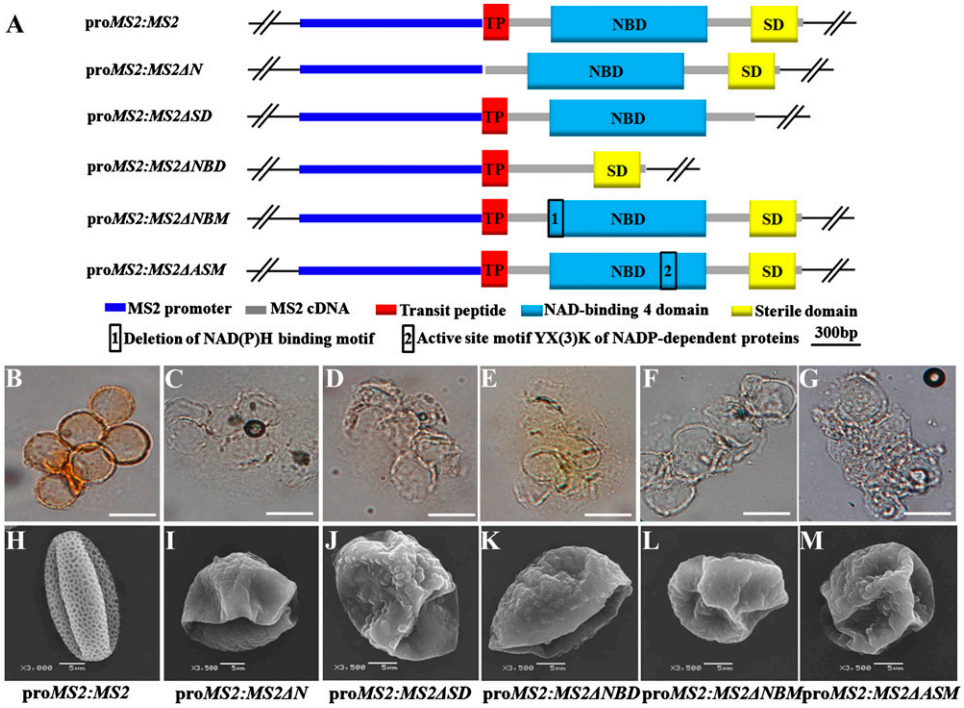

Figure 4. Functional complementation of the *ms2* mutant using truncated *MS2* cDNA fragments. A, Diagrams of the constructs of the full-length *MS2* cDNA under the control of the *MS2* promoter (pro*MS2*:*MS2*), *MS2* cDNA without the sequence encoding the putative transit peptide (pro*MS2*:*MS2ΔN*), *MS2* cDNA without the sequence encoding the SD (pro*MS2*:*MS2ΔSD*), *MS2* cDNA without the sequence encoding the NAD-binding 4 domain (pro*MS2*:*MS2ΔNBD*), *MS2* cDNA without the sequence encoding the NAD(P)H-binding motif (pro*MS2*:*MS2ΔNBM*), and *MS2* cDNA without the sequence encoding the active site motif YX(3)K of NADP-dependent proteins (pro*MS2*:*MS2ΔASM*). B to M, These constructs were transformed to the *ms2* mutants individually, and pollen grains were detected by acetolysis treatment (B–G) and SEM analysis (H–M). Bars = 20 μm (B–G) and 5 μm (H–M). [See online article for color version of this figure.]

homozygous mutants, whereas pro*M2*:*MS2* rescued the defect of *ms2* pollen wall development (Fig. 4, A, B, C, H, and I). The Arabidopsis Rubisco small subunit protein contains an N-terminal transit peptide (RTP) that has been shown to effectively target this protein to chloroplasts (Kim et al., 2010a). To test whether RTP can functionally replace the N-terminal transit peptide of MS2 protein, we made the construct pro*MS2*:*RTP-MS2*△*N′*, in which the fragment of *RTP* translationally replaced the N-terminal transit peptide of MS2 (Fig. 5A) and transformed it to *ms2* mutants. Twenty-one independent transgenic lines containing pro*M2*:*RTP-MS2ΔN′* in the *ms2* homozygous background were obtained. Acetolysis treatment and SEM analysis showed that 10 transgenic lines displayed normal pollen exine development compared with the wild type (Fig. 5, B and E), suggesting the rescued pollen wall phenotype of *ms2* mutants by this construct. The pollen grains of four transgenic lines showed partially resistant to acetolysis treatment and less defective outer surface analyzed by SEM, suggesting a partially rescued phenotype of pollen exine formation (Fig. 5, C and F). Seven transgenic lines showed defects of pollen exine development similar to *ms2* (Fig. 5, D and G), which may have resulted from the difference between the RTP and the N-terminal transit peptide of MS2. These results confirmed that the localization of MS2 to plastids is critical for its function in anther development.

NAD(P)H-Binding Domain and Sterile Domain Are Essential for MS2 Function

Consistent with a previous investigation (Aarts et al., 1997), analysis of the MS2 protein using the SMART protein structure prediction tool (http://smart.embl-heidelberg.de/) revealed that the MS2 protein contains two conserved domains: the NAD(P)H-binding domain (NBD) between residues 135 and 438 and the sterile domain (SD) between residues 534 and 614.

MS2 and other FARs were observed to contain the conserved NAD(P)H-binding motif between residues 133 and 143 [(I/V/F)X(I/L/V)TGXTGFL(G/A)] and the active site motif YX(3)K of NADP-dependent proteins between residues 357 and 368 (Fig. 4A; Aarts et al., 1997; Doan et al., 2009), implying a functional role of these motifs.

To examine whether these domains/motifs are essential for MS2 function, we made several constructs containing the mutated *MS2* fragments driven by the *MS2* promoter (Fig. 4A). The construct containing the deleted SD sequence (pro*MS2*:*MS2*△*SD*) or deletion of the NBD domain (pro*MS2*:*MS2*△*NBD*) could not rescue the defective pollen exine development in the *ms2* homozygous background (Fig. 4, A, D, E, J, and K), suggesting an essential role of both SD and NBD domains in MS2 function. Furthermore, the constructs deleted for the NAD(P)H-binding motif or the active site motif YX(3)K of NADP-dependent proteins failed to complement the defective pollen exine phenotype of *ms2* in the transgenic plants (Fig. 4, A, F, G, L, and M), suggesting the essential role of these two conserved motifs in the NBD of MS2.

Purified Recombinant MS2 Enzyme Has Fatty Acyl-ACP Reductase Activity

Although MS2 is predicted as a fatty acid reductase involved in fatty alcohol formation and recombinant bacteria expressing MS2 can produce C14:0, C16:0, and C18:1 alcohols (Aarts et al., 1997; Doan et al., 2009), a comprehensive biochemical characterization of this enzyme has not been performed. To this end, we cloned the full-length *MS2* cDNA into the expression vector pET30a (Novagen) and introduced it into *E. coli* BL21 (DE3). The recombinant MS2 protein was purified by affinity chromatography and subjected to SDS-PAGE. Compared with the predicted size of about 73 kD, the molecular mass of the affinity-purified protein ran somewhat faster on SDS-PAGE (Fig. 6).

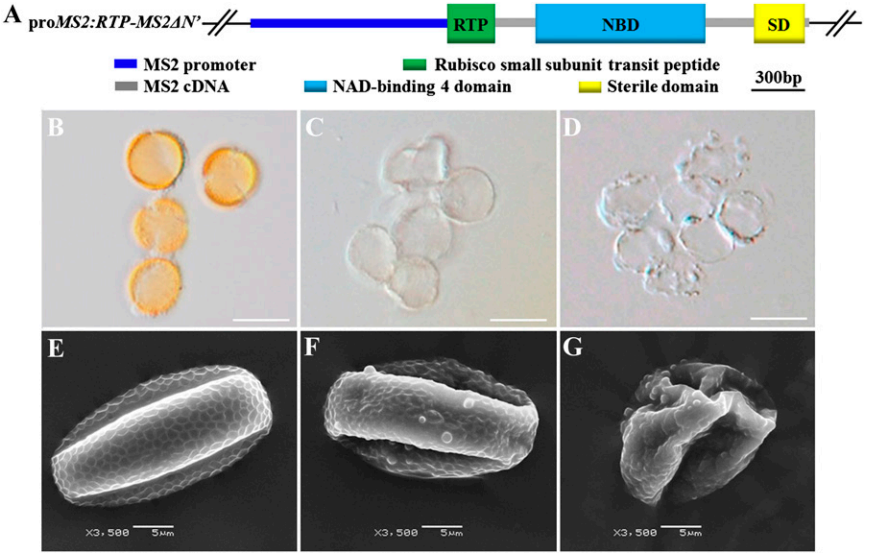

Figure 5. Complementation analysis of the *ms2* mutant using the truncated *MS2* fused with the DNA fragment encoding the Arabidopsis RTP. A, Diagrams of the construct of the *MS2* cDNA containing the fragment encoding the Arabidopsis RTP replacing the fragment encoding the MS2 N-terminal transit peptide under the control of the *MS2* promoter (pro*MS2*:*RTP-MS2ΔN′*). Ten transgenic lines could well restore the pollen phenotype of the *ms2* mutant (B and E); four transgenic lines could only partly restore the pollen phenotype of the *ms2* mutant (C and F); seven transgenic lines could not restore the pollen phenotype of the *ms2* mutant (D and G). B to D, Analysis of acetolysis treatment. E to G, SEM analysis. Bars = 20 μm (B–D) and 5 μm (E–G). [See online article for color version of this figure.]

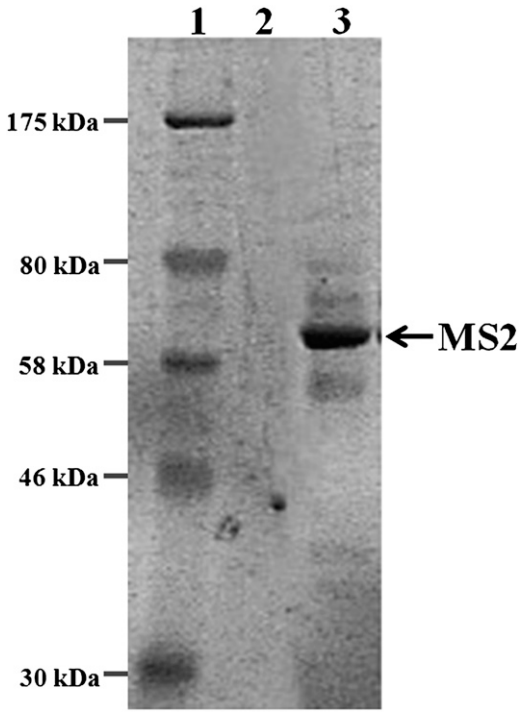

Figure 6. Analysis of Ni^{2+}-NTA column affinity-purified MS2. Lane 1, prestained protein markers; lane 2, 10 μL of eluted solution from the Ni^{2+}-NTA affinity column incubated with the protein from control bacteria containing the empty vector pET30a; lane 3, 10 μL of purified His tag fused-*MS2* protein from the Ni^{2+}-NTA affinity column incubated with protein from pET30a-MS2.

Because the data presented herein show that MS2 is localized in plastids in which long-chain fatty acids are de novo synthesized and while esterified to ACP (Li-Beisson et al., 2010), we analyzed MS2 activity with acyl-ACPs. Using ^{14}C-labeled fatty acyl-ACPs, we detected strong activity only with [1-^{14}C]16:0-ACP, trace activity with [1-^{14}C]18:0-ACP, and no activity with [1-^{14}C]14:0-ACP, [1-^{14}C]16:1-ACP, and [1-^{14}C]18:1-ACP (Supplemental Table S1), indicating that MS2 prefers palmitoyl-ACP as a substrate. Furthermore, no activity was detected with the equivalent [1-^{14}C]acyl-CoA substrates (data not show). To further investigate the substrate specificity of recombinant MS2, unlabeled myristoyl-ACP, palmitoyl-ACP, palmitoleoyl-ACP, and stearoyl-ACP were tested with the purified MS2 enzyme in the presence of NAD(P)H, and only palmitoyl-ACP was reduced to C16:0 alcohol (Fig. 7). The specificity of MS2 against palmitoyl-ACP was confirmed by using deuterium-labeled 7,7,8,8-d_4-palmitoyl-ACP as substrate, which yielded a product at the same retention time as hexadecanol but with a mass ion +4 relative to the non-mass-labeled standard (Supplemental Fig. S2).

To more comprehensively characterize the MS2 enzyme, we compared the palmitoyl-ACP-reducing activity in the presence of NAD(P)H versus NADH. Under the same experimental conditions, chromatographic analysis revealed that the recombinant MS2 has higher activity in the presence of NAD(P)H relative to that using NADH, and no C16:0 alcohol was detectable if NAD(P)H or NADH was omitted (Fig. 8), suggesting that MS2 activity is dependent on the presence of either NAD(P)H or NADH. Furthermore, we show that the optimal pH value for the MS2 activity is 6.0 (Fig. 9). Additionally, assays at various temperatures showed that the optimal working temperature for the MS2 converting palmitoyl-ACP to the C16:0 alcohol is 30°C (Fig. 9). Under the condition of optimum pH and temperature, the recombinant MS2 has a K_m of 23.3 $\pm$ 4.0 μM for palmitoyl-ACP and a V_{max} of 38.3 $\pm$ 4.5 nmol mg^{-1} min^{-1} (Table I).

Fatty Alcohol Production in Tobacco Leaves Transiently Expressing MS2

To demonstrate the physiological role of MS2 activity in producing fatty acyl alcohols, we transiently expressed the MS2 protein in tobacco leaves using a cowpea mosaic virus RNA-2-based expression system (Sainsbury and Lomonossoff, 2008). The constructed

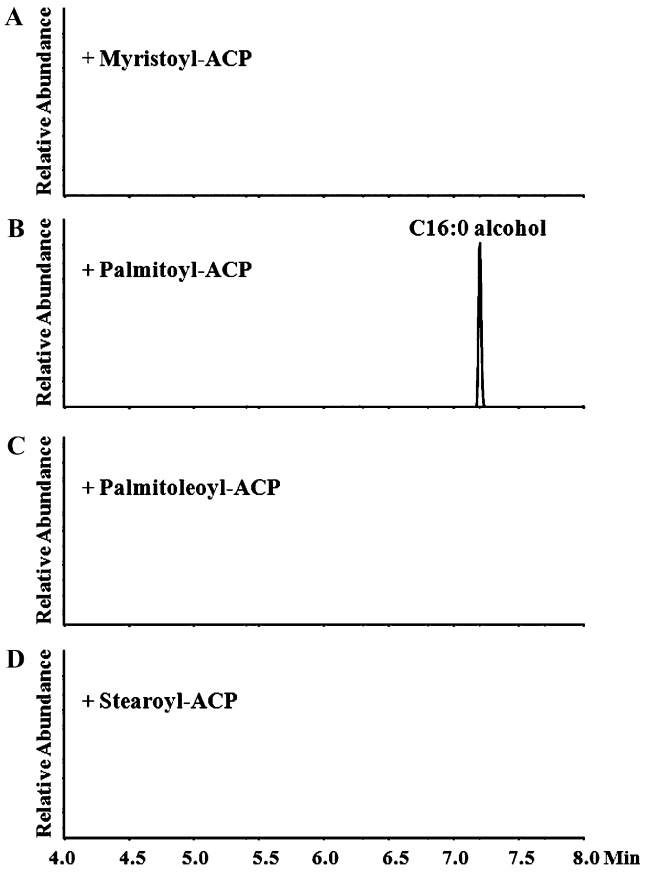

Figure 7. Substrate specificity analysis of recombinant MS2. Gas chromatograms of metabolites generated from the incubation of myristoyl-ACP (A), palmitoyl-ACP (B), palmitoleoyl-ACP (C), and stearoyl-ACP (D) with affinity-purified MS2 in the presence of NAD(P)H are shown.

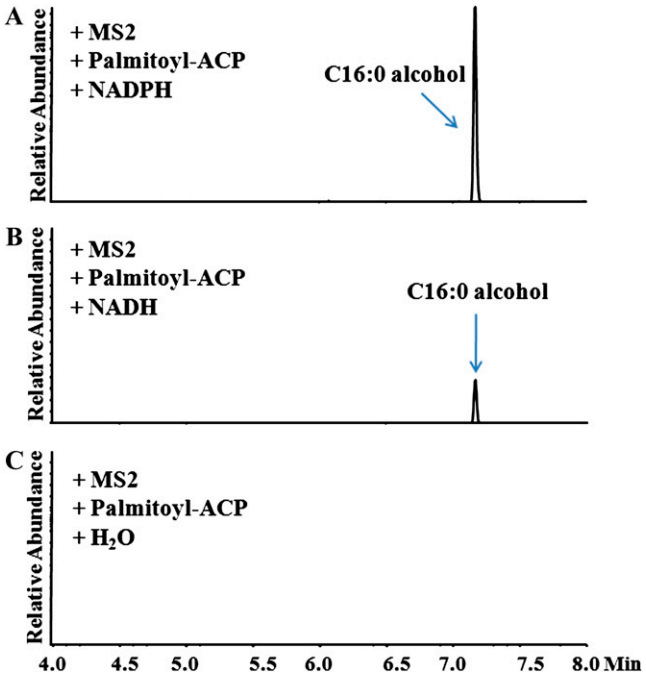

Figure 8. Catalytic activity analysis of MS2 dependent on NAD(P)H and NADH. Gas chromatograms of products generated with incubations of 20 μM palmitoyl-ACP with purified MS2 in the presence of NAD(P)H (A), NADH (B), or water (C) are shown. [See online article for color version of this figure.]

vector p*EAQ*:*MS2* was transformed into tobacco leaves, and overexpression of MS2 protein was confirmed by western-blot analysis using an MS2-specific antibody (see "Materials and Methods") of the tobacco leaf extracts 3 d after *Agrobacterium tumefaciens* infiltration (Supplemental Figs. S3 and S4). The lipidic compositions of chloroform-extractable cuticular waxes, cutin monomers, and total soluble lipids were analyzed in the transgenic lines using gas chromatography-mass spectrometry (GC-MS) and gas chromatography-flame ionization detection (GC-FID; Bonaventure et al., 2004; Franke et al., 2005) and compared with lines carrying the empty vector p*EAQ* as the control.

From GC-FID analysis, we observed that the amounts of total wax and total soluble lipids per cm^2 of tobacco leaves in the p*EAQ*:*MS2* lines were very close to those of the control lines. In contrast, the total cutin amount per cm^2 of tobacco leaves was significantly higher in the p*EAQ*:*MS2* lines compared with the control lines (Fig. 10A). Interestingly, compared with the control lines, significant increases of the contents of hexacosanol, octadecanol, and C29 alkane were observed in the wax of tobacco leaves harboring p*EAQ*:*MS2* (Fig. 10B; Supplemental Table S2) as well as increased levels of hexacosanol and C20 fatty acid in internal lipids (Fig. 10C; Supplemental Table S3). In addition, significant accumulations of hexacosanol, octadecanol, octadecanoic acid, oleic acid, eicosanoic acid, docosanoic acid, and unknown cutin monomer were observed in the cutin monomers of the transgenic tobacco leaves (Fig. 10D; Supplemental Table S4). These results suggested that MS2 can synthesize fatty alcohols in plants.

DISCUSSION

MS2 Encodes a Fatty Acyl-ACP Reductase Essential for Normal Pollen Exine Development

Male reproductive development in higher plants is indispensable for the synthesis of fatty acid derivatives (Li and Zhang, 2010). Our results show that purified recombinant MS2 is able to produce C16:0 alcohol, which is required for pollen exine development. Although the biochemical nature of pollen exine remains exclusive, we previously showed that pollen exine may share a common lipidic biosynthetic pathway with that of cutin, which is an insoluble polymer matrix containing the major constituents of hydroxylated and epoxy hydroxylated C16 and C18 fatty acids as well as minor components such as fatty alcohols (Li et al., 2010; Zhang et al., 2010). Fatty alcohols with C16 and C18 occupy 0% to 8% of cutin composition (Pollard et al., 2008). CYP704B2 belongs to a conserved and ancient subfamily of fatty acid hydroxylases and is specifically expressed in the tapetum and the microspore. Mutation of CYP704B2 causes aborted pollen

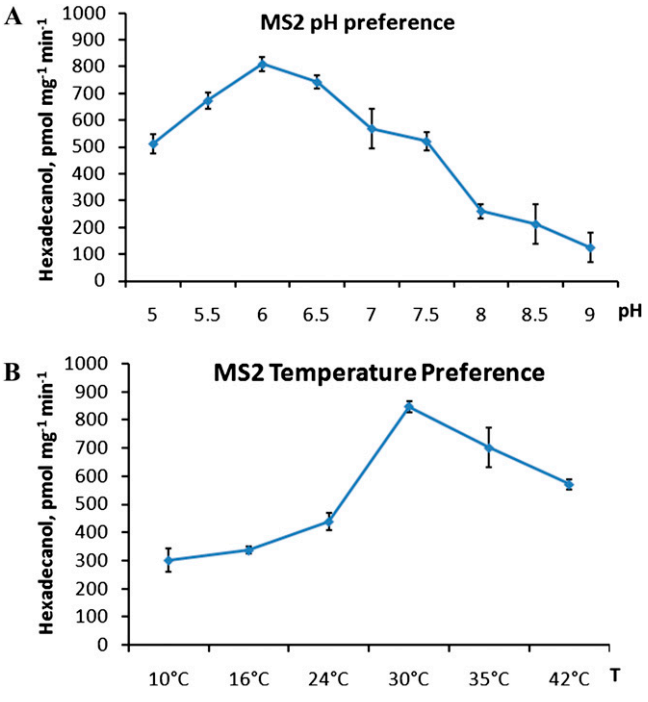

Figure 9. pH and temperature preferences of recombinant MS2. Activity analyses of the recombinant MS2 with the pH range 5.0 to 9.0 (A) and using the optimum MES buffer (pH 6.0) incubated at 10°C, 16°C, 25°C, 30°C, 35°C, and 42°C (B) are shown. The values indicate means of four replicates ± SD. [See online article for color version of this figure.]

Table I. *Kinetic properties of MS2 catalyzing palmitoyl-ACP*

Enzyme activity was measured by the assay with affinity-purified MS2 protein and various concentrations of palmitoyl-ACP. Catalytic efficiency (k_{cat}) means and SE values are based on four replicates.

K_m	V_{max}	k_{cat}	k_{cat}/K_m
μM	*nmol* mg^{-1} min^{-1}	s^{-1} 10^{-3}	M^{-1} s^{-1}
23.3 ± 4.0	38.3 ± 4.5	43.6 ± 5.1	1,873 ± 218

grains without detectable exine and undeveloped anther cuticle with reduced levels of cutin monomers. Recombinant CYP704B2 catalyzes the production of ω-hydroxylated fatty acids with 16 and 18 carbon chains, suggesting that CYP704B2 is involved in the biosynthesis of the two biopolymers sporopollenin and cutin (Li et al., 2010). Accordingly, we propose that the MS2-derived fatty alcohol may account for pollen exine development. Consistently, we recently genetically characterized a close homolog of MS2 in rice called Defective Pollen Wall (DPW). *dpw* displays defective anther development and aborted pollen grains with an abnormal exine, causing complete male sterility. Additionally, *dpw* anthers have significantly reduced levels of cutin monomers and cuticular wax composition as well as soluble fatty acids and alcohols (Shi et al., 2011). *dpw*, like MS2, is able to produce C16 primary alcohols.

MS2 has a spatiotemporal expression pattern in tapetal cells (Aarts et al., 1997; Fig. 3) that is consistent with the tapetal role in synthesizing and secreting lipidic sporopollenin precursors (Li and Zhang, 2010). This expression pattern is similar to other tapetum-expressed genes, such as the fatty acid-metabolizing genes *CYP703s* (Morant et al., 2007; Aya et al., 2009), *ACOS5* (de Azevedo Souza et al., 2009), *CYP704Bs* (Dobritsa et al., 2009; Li et al., 2010; Yi et al., 2010), *TKPR1/2* (Grienenberger et al., 2010), and *LAP6/PKSA* and *LAP5/PKSB* (Tang et al., 2009; Dobritsa et al., 2010; Kim et al., 2010b) as well as *WBC27/ABCG26* (Quilichini et al., 2010; Xu et al., 2010; Choi et al., 2011; Dou et al., 2011), *OsC6* (Zhang et al., 2010), and *DPW* (Shi et al., 2011).

In this study, we show that the purified recombinant MS2 has a strong preference for converting palmitoyl-ACP to hexadecanol that is dependent on the electron donor NAD(P)H, but it can also use NADH with lower efficiency. Compared with previous investigations, this study provides biochemical insight into plastidially localized enzymes with sequence homology to the FARs from the green alga *Euglena gracilis* (Kolattukudy, 1970), jojoba (Metz et al., 2000), oilseed rape (*Brassica napus*; Hu et al., 2006), and Arabidopsis (Rowland et al., 2006; Doan et al., 2009; Domergue et al., 2010). In the Arabidopsis genome, eight FAR-like sequences were identified, and five FARs have been biochemically investigated (Doan et al., 2009). The Arabidopsis FARs share sequence similarity with the jojoba FAR (30% to 54% identity), and CER4 has the highest sequence identity to that of jojoba (54%; Doan et al., 2009). Yeast cells expressing Arabidopsis CER4 generated C24:0 and C26:0 primary alcohols, and CER4 is required for the development of epidermal cells of aerial organs and roots (Rowland et al., 2006). Bacteria expressing MS2 are capable of producing C14:0, C16:0, and C18:1 alcohols (Doan et al., 2009). We are currently unable to reconcile this observation with our biochemical assays, in which we failed to detect activity with [1-^{14}C]C14:0 substrates. It is possible that bacteria expressing MS2 have more complex metabolic activities mediated by MS2 and bacterial enzymes that are not revealed in purified enzyme assays. Unlike MS2, the FAR enzyme from jojoba is able to convert acyl-CoAs to C16:0 and C18:0 fatty alcohols, which are required for wax production in jojoba seeds (Metz et al., 2000). Silk moth FAR-expressing yeast cells could convert C14-20 fatty acids to alcohols and preferentially to C15 and C16 fatty acids (Moto et al., 2003). Two mouse enzymes, FAR1 and FAR2, were shown to reduce fatty acyl-CoA ester substrates into fatty alcohols (Cheng and Russell, 2004). Unlike the recombinant MS2, the recombinant DPW can convert both palmitoyl-ACP and palmitoyl-CoA into hexadecanol despite its higher activity to palmitoyl-ACP (Shi et al., 2011). In addition, the K_m value of the recombinant MS2 toward palmitoyl-ACP was determined to be about 6.5-fold higher than that of DPW, suggesting that DPW has higher affinity for palmitoyl-ACP than MS2. Moreover, the recombinant MS2 has trace activity against [1-^{14}C]18:0-ACP that is not detectable for DPW. Furthermore, the DPW activity depends exclusively on NAD(P)H (Shi et al., 2011), whereas MS2 can use either NAD(P)H or NADH. These results suggest that MS2 homologs have undergone substantial diversification during the course of the evolution of monocots and dicots.

Alignment analysis revealed that MS2, DPW, and FARs from Arabidopsis (CER4), jojoba, wheat (TAA1a), silk moth, and mouse share conserved NAD(P)H-binding and active site motifs (Doan et al., 2009; Shi et al., 2011). In this study, we demonstrate the biological importance of these motifs in anther development by genetic complementation (Fig. 4), implying that these motifs are essential for enzyme function. In addition, the critical role of the SD conserved in MS2 and other homologs (Aarts et al., 1997) was also empirically demonstrated in this investigation (Fig. 4).

MS2 Represents a Conserved Plastid-Localized Lipid Metabolism Pathway That Operates during Anther Development

Plant anther cells contain various types of diversified plastids, and plastids within tapetal cells are thought to be associated with lipid synthesis and secretion for pollen wall synthesis (Clement and Pacini, 2001). Plant de novo biosynthesis of fatty acids with short carbon chain lengths of up to C18 is mainly in plastids (Ohlrogge et al., 1979; Li-Beisson et al., 2010). We revealed that the MS2/DPW protein is localized to chloroplasts, and a genetic complementation assay shows that the

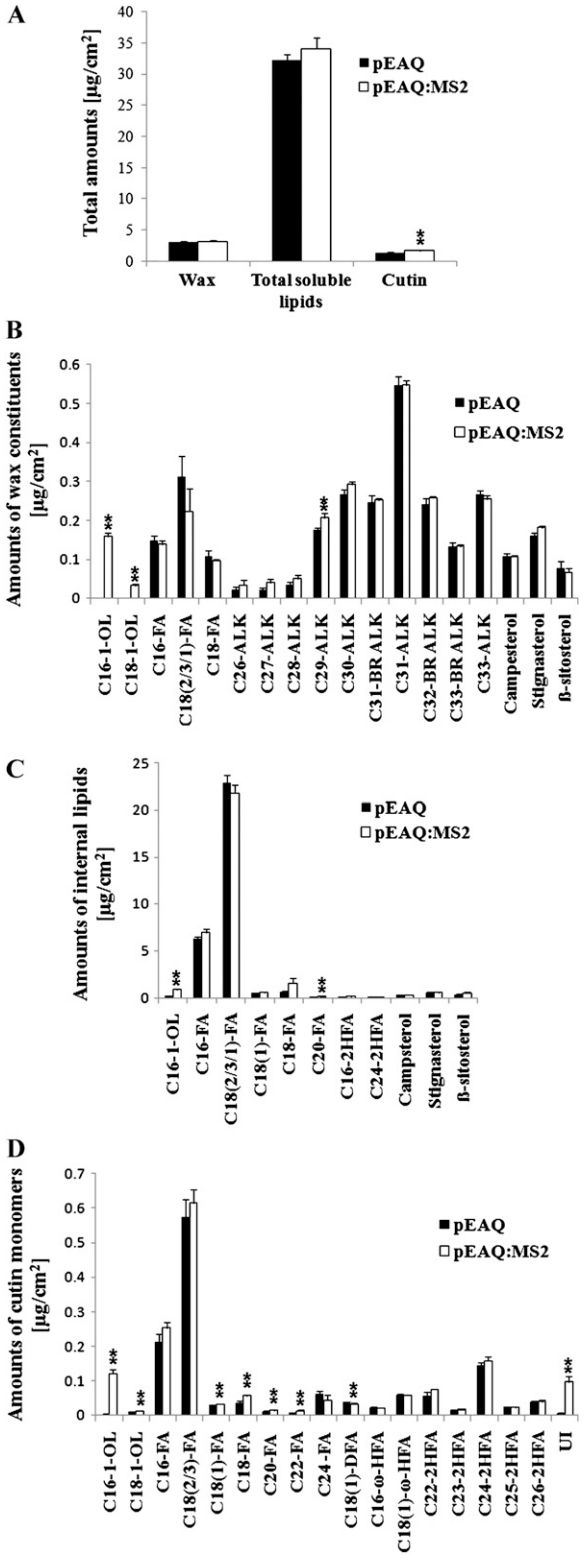

Figure 10. Analysis of wax, internal lipids, and cutin in transient tobacco leaves. A, Total wax, internal lipids, and cutin amounts per unit surface area (mg cm^{-2}) in tobacco leaves by transient expression of MS2 (white bars) or empty vector (black bars). B, Wax constituent amounts per unit surface area (mg cm^{-2}) in tobacco leaves by transient expression of MS2 (white bars) or empty vector (black bars). C, Internal lipid amounts per unit surface area (mg cm^{-2}) in tobacco leaves by transient expression of MS2 (white bars) or empty vector (black bars). D, Cutin monomer amounts per unit surface area (mg cm^{-2}) in tobacco leaves by transient expression of MS2 (white bars) or empty vector (black bars). The values indicate means of five biological replicates ± SD. ** $P < 0.01$. Compound names are as follows: C16-1-OL, hexacosanol; C18-1-OL, octadecanol; C16-FA, hexadecanoic acid; C18-FA, octadecanoic acid; C18(2/3)-FA, linoleic and linolenic acid; C18(1)-FA, oleic acid; C20-FA, eicosanoic acid; C22-FA, docosanoic acid; C24-FA, etracosanoic acid; C16-2HFA, 2-hydroxy-hexadecanoic acid; C23-2HFA, 2-hydroxy-tricosanoic acid; C24-2HFA, 2-hydroxy-tetracosanoic acid; C25-2HFA, 2-hydroxy-pentacosanoic acid; C26-2HFA, 2-hydroxy-hexacosanoic acid; C16-ω-HFA, 16-hydroxyhexadecanoic acid; C18(1)-ω-HFA, 18-hydroxy-octadecanoic acid; C18(1)-DFA, octadecene-1,18-dioic acid; UI, unknown cutin monomer; ALK, alkane; BR, branched aliphates.

N-terminal transit peptide is required for the MS2/DPW function in anther development (Figs. 4 and 5; Shi et al., 2011). A similar N-terminal transit peptide is also observed in other MS2 homologs (Doan et al., 2009; Shi et al., 2011). Therefore, our data show that a plastid-localized and conserved pathway of converting fatty acids to fatty alcohols is required for male reproductive development in monocots and dicots (Shi et al., 2011).

In conclusion, we have characterized an Arabidopsis plastid-localized fatty acyl-ACP reductase, MS2, that is able to reduce palmitoyl-ACP to C16:0 alcohol. The plastidial MS2 fatty alcohol production pathway is essential for pollen exine synthesis. Moreover, the subcellular localization of MS2 in plastids, mediated by its N-terminal transit peptide, NBD, and SD and the active site motif YX(3)K, is required for MS2 function in anther development. This work reveals a key and conserved step of primary fatty alcohol synthesis for pollen wall biosynthesis in Arabidopsis.

MATERIALS AND METHODS

Plant Materials and Growth Conditions

Arabidopsis (*Arabidopsis thaliana* Columbia ecotype) plants were grown in a greenhouse at 22°C and 70% relative humidity under continuous illumination. The *ms2* mutant, a T-DNA insertion line (SAIL_92_C07), was obtained from the Arabidopsis Biological Resource Center. Tobacco (*Nicotiana benthamiana*) plants were grown in a greenhouse at 25°C with 16 h of supplemental light per day.

Staining, SEM, and Acetolysis Treatment

For DAPI staining, pollen grains were fixed in formaldehyde acetic acid, immersed in 0.2% DAPI, and viewed by fluorescence microscopy under UV light (Leica DM2500). For I_2-KI staining, pollen grains were immersed in I_2-KI solution and photographed with a microscope (Leica DM2500). For SEM, pollen grains were air dried in silica, coated with palladium-gold in a sputter coater (Hummer), and then observed in an autoscan scanning electron microscope (JEOL) with an acceleration voltage of 30 kV. Acetolysis treatment was performed as described previously (Aarts et al., 1997).

Laser Scanning Confocal Microscopy

The Arabidopsis protoplasts were prepared and transformed as described (Yoo et al., 2007). Tobacco leaf cells were observed 2 d after argoinfiltration in 50% glycerol. Fluorescence was detected by a Leica TCS SP5 confocal laser scanning microscope with an argon laser at 488 nm for excitation and images for GFP and chlorophyll signals and at 543 nm for mitochondria marker F1ATPase-γ-RFP. The signals were collected from 505 to 525 nm for GFP, 650 to 750 nm for chlorophyll, and 560 to 620 nm for F1ATPase-γ-RFP.

Vector Construction

The *MS2* promoter fragment (1,095-bp upstream fragment of the start codon ATG) was amplified from wild-type Arabidopsis genomic DNA with the primers MS2pro-F and MS2pro-R and cloned into the binary vector pCAMBIA1301 to generate vector p1301proMS2. The full-length *MS2* cDNA (1,851 bp) was amplified from wild-type Arabidopsis inflorescence cDNA with the primers MS2-1F/1R and cloned into pMD 18-T vector (Novagen). For deletion analysis of the *MS2* gene, serial primers were used to amplify *MS2*, *MS2ΔN*, *MS2ΔSD*, *MS2ΔNADP*, *MS2ΔNBM*, and *MS2ΔASM* fragments, which were then digested with *Nco*I and *Bst*EII and subcloned into the vector under the control of the *MS2* promoter, named pro*MS2*:*MS2*, pro*MS2*:*MS2ΔN*, pro*MS2*:*MS2ΔSD*, pro*MS2*:*MS2ΔNBD*, pro*MS2*:*MS2ΔNBM*, and pro*MS2*:*MS2ΔASM*, respectively.

For the analysis of MS2 subcellular localization, two *MS2* fragments (a 1,848-bp full-length cDNA without the stop codon TAA [*MS2*] and a 1,701-bp truncated cDNA lacking the 147-bp fragment encoding the N-terminal transit peptide and the stop codon TAA [*MS2ΔN*]) were amplified with primers MS2-1F/2R and MS2ΔN-F/MS2-2R, respectively. The *GFP* coding region was amplified with primers GFP-F/R. *MS2* or *MS2ΔN* (digested with *Nco*I and *Bgl*II) and *GFP* (digested with *Bgl*II and *Bst*EII) were subcloned into pMS2 or pCAMBIA 1301 (previously digested with *Nco*I and *Bst*EII) to generate pro*MS2*:*MS2-GFP*, pro*MS2*:*MS2ΔN-GFP*, pro*35S*:*MS2-GFP*, and pro*35S*:*MS2ΔN-GFP*. The N-terminal transit peptide-encoding sequence of *MS2* was amplified using primers TP-F/R, digested with *Sal*I and *Spe*I, and cloned into p*A7-YFP* (kindly provided by Prof. Hongquan Yang) to generate pro*35S*:*TP-YFP*. The DNA fragment encoding the Arabidopsis RTP (240 bp; GenBank accession no. AT1G67090) was amplified from wild-type Arabidopsis inflorescence cDNA with the primers RTP-F/R. The amplified *RTP* was fused to the N terminus of the truncated *MS2* fragment (1,761 bp, encoding MS2 residues 31–616) using overlapping PCR with the primers MS2ΔN2-F and MS2-1R; the resulting fragment was digested with *Nco*I and *Bst*EII and then cloned into pro*MS2*, generating pro*MS2*:*RTP-MS2ΔN′*.

For overexpressing *MS2*, the *MS2* fragment was amplified with the primers MS2-2F/3R and cloned into the *Age*I- and *Xho*I-digested p*EAQ* (Sainsbury and Lomonossoff, 2008) to generate p*EAQ*:*MS2*. For preparation of the MS2 antibody, the specific MS2 fragment with less similarity to other Arabidopsis genes was amplified with primers MS2f-1F/1R and MS2f-2F/2R. The two PCR products were cloned into the *Bam*HI and *Xho*I sites of pET30a, forming p*ET30a*:*MS2S*. For expression of the MS2 enzyme in *Escherichia coli*, the *MS2* fragment was amplified with primers MS2-3F/3R and cloned into pET30a (Novagen) digested with *Bam*HI and *Sal*I, resulting in p*ET30a*:*MS2*.

All constructs were confirmed by sequencing. Sequences of the primers used are listed in Supplemental Table S5.

Transformation

Constructs pro*MS2*:*MS2*, pro*MS2*:*MS2ΔN*, pro*MS2*:*MS2ΔSD*, pro*MS2*:*MS2ΔNBD*, pro*MS2*:*MS2ΔNBM*, pro*MS2*:*MS2ΔASM*, and pro*MS2*:*RTP-MS2ΔN′* were individually introduced into *Agrobacterium tumefaciens* GV3101 and transformed into *ms2* mutants. Constructs pro*MS2*:*MS2-GFP* and pro*MS2*:*MS2ΔN-GFP* were individually introduced into *A. tumefaciens* GV3101 and transformed into wild-type plants. Transgenic plants were screened with hygromycin selection and confirmed by PCR. Constructs pro*35S*:*MS2-GFP* and pro*35S*:*MS2ΔN-GFP*, p*EAQ*, and p*EAQ*:*MS2* were introduced into *A. tumefaciens* EHA105 individually and transformed into tobacco using the method of He et al. (2008).

Polyclonal Antibody Preparation and Western Blot

p*ET30a*:*MS2S* was transformed into BL21 (DE3) *E. coli* cells, and the recombinant cells were grown at 37°C in Luria-Bertani medium containing 50 mg L^{-1} kanamycin to an optical density at 600 nm of 0.8 and induced using 1 mM isopropyl β-D-1-thiogalactopyranoside. After 48 h of induction at 20°C, the cell pellet was collected by centrifugation at 4°C. The fusion protein purification and antibody preparation were performed as described by Huang et al. (2003). The antiserum was collected after four injections. The antibody was purified according to the method described by Ritter (1991).

Total soluble proteins were extracted from the wild-type buds and p*EAQ*- and p*EAQ*:*MS2*-transformed tobacco leaves using the protocol described by Huang et al. (2003) and separated by 10% SDS-PAGE. After electrophoresis, the proteins were electronically transferred onto nitrocellulose membranes and incubated with the purified antibodies (1:100 dilution) as described by Huang et al. (2003).

Expression, Purification, and Activity Assay of Recombinant MS2

BL21 (DE3) *E. coli* cells containing p*ET30a*:*MS2* were grown at 30°C to an optical density at 600 nm of 0.6, and MS2 expression was induced by the addition of 0.5 mM isopropyl β-D-1-thiogalactopyranoside and further incubation at 20°C for 48 h. The cell pellet was collected by centrifugation at 4°C and resuspended in phosphate-buffered saline buffer (137 mM NaCl, 2.7 mM KCl, 8.1 mM Na_2HPO_4, and 1.76 mM KH_2PO_4, pH 7.4) containing 1 mM phenylmethylsulfonyl fluoride and 5 mM dithiothreitol and then lysed by French press. The lysis solution was clarified by centrifugation (45,000*g*) and loaded onto a nickel-nitrilotriacetic acid agarose (Ni^{2+}-NTA) affinity column (Merck) following the manufacturer's instructions. The bound proteins were eluted with phosphate-buffered saline containing 70 mM imidazole and detected by 10% SDS-PAGE. Nonspecific proteins purified from pET30a-transformed bacteria were used as a negative control.

C16:0-ACP, 7,7,8,8-d_4-C16:0-ACP, C14:0-ACP, C18:0-ACP, C16:1-ACP, [1-^{14}C]14:0-ACP, [1-^{14}C]16:0-ACP, [1-^{14}C]16:1-ACP, [1-^{14}C]18:0-ACP, and [1-^{14}C]18:1-ACP were synthesized enzymatically (Rock and Garwin, 1979) using recombinant spinach (*Spinacia oleracea*) ACP-I (Broadwater and Fox, 1999). For the substrate preference analysis using unlabeled fatty acyl-ACP, the reductase activity of MS2 was analyzed as described by Metz et al. (2000). The reaction mixture of 200 μL for the MS2 assay contained 15 mM NAD(P)H, 25 mM HEPES-NaOH, pH 7.5, 1 mM dithiothreitol, 1 mM EDTA, 10% (w/v) glycerol, and 0.3% (w/v) CHAPS plus the desired substrate. NAD(P)H was replaced by NADH or water for the catalytic activity analysis of MS2. The reaction was initiated by addition of the enzyme, and for negative control experiments, an equivalent volume of eluted buffer from the Ni^{2+}-NTA column that had been incubated with protein from cells expressing the empty pET30a vector was added. Incubations were performed at 30°C for 60 min and terminated by the addition of an equal volume of cyclohexane. The products were extracted into 1.2 volumes of hexane, and 2 μL of this extract was subjected to GC-MS analysis.

The Agilent GC apparatus was coupled with an Agilent 5975C inert XL MSD with triple axis detector. The detector and injector temperature were maintained at 300°C. The oven temperature of 120°C was increased to 240°C at a rate of 15°C min^{-1} and held at 240°C for 2 min.

For substrate preference with ^{14}C-labeled fatty acyl-ACPs, the 150-μL reaction was carried out as described above and incubated at 30°C for 30 min. For pH optimization, 50 mM MES/50 mM Bis-Tris propane buffer with pH range from 5.0 to 9.0 was used, and the reaction was incubated for 15 min. For temperature optimization, the optimum MES buffer (pH 6.0) was used and incubated at 10°C, 16°C, 25°C, 30°C, 35°C, and 42°C. For kinetics analysis of MS2 using [1-^{14}C]16:0-ACP, the reaction was carried out at optimum pH (50 mM MES, pH 6.0) and temperature (30°C) for 10 min. The reactions were extracted twice with 2 volumes of hexane. The radioactivity of the hexane fraction was measured by liquid scintillation counting. As described above, extracts from bacteria expressing pET30a were used as the negative control.

Analysis of Wax, Internal Lipids, and Cutin in Tobacco Leaves

Tobacco leaf discs used for the analysis of wax, internal lipids, and cutin were prepared as described (Cameron et al., 2006) with modifications. Leaf discs (1.5 cm diameter) were excised using a cork borer from the leaves 3 d after argoinfiltration of p*EAQ* or p*EAQ*:*MS2*, frozen immediately in liquid N_2, freeze dried, and then stored in silica gel at room temperature. Each sample contained six leaf discs derived from three individual plants.

Cuticular waxes were extracted from the leaf discs described above by immersing tissues for 30 s in 1 mL of chloroform containing 10 μg of

tetracosane (Fluka) as an internal standard. The extracts were transferred to reactive vials and dried under a gentle stream of nitrogen gas. The dried wax residues were derivatized by adding 20 μL of *N*,*N*-bis-trimethylsilyltrifluoroacetamide (Macherey-Nagel) and 20 μL of pyridine and incubated for 40 min at 70°C. These derivatized samples were then analyzed by GC-FID (Agilent Technologies) and GC-MS (Agilent gas chromatograph coupled to an Agilent 5973N quadrupole mass selective detector).

For total internal lipid extraction, leaf discs that had been used in the wax extraction were reextracted with 1 mL of chloroform:methanol (1:1, v/v). They were first incubated at 50°C for 30 min and then overnight with constant shaking at room temperature. This extraction was repeated three times to ensure that no internal lipids were left in the samples. The combined lipid extracts were then dried under a gentle stream of nitrogen gas to about 100 μL. The remaining delipidated leaf discs were dried over silica gels and used to analyze the monomer composition of cutin polyester as described by Franke et al. (2005). All internal lipid samples and cutin samples were trans-esterified in 1 mL of 1 N methanolic HCl for 2 h at 80°C. After the addition of 2 mL of saturated NaCl and 20 μg of dotriacontane (Fluka) as an internal standard, the hydrophobic monomers were subsequently extracted three times with 1 mL of hexane. The organic phases were combined and dried under a stream of nitrogen gas, and the remaining samples were derivatized as described above. GC-MS and GC-FID analyses were performed as for the wax analysis. Results of leaf wax, internal lipids, and cutin analyses were expressed relative to unit surface area of tobacco leaves.

Supplemental Data

The following materials are available in the online version of this article.

Supplemental Figure S1. Subcellular localization of MS2 in tobacco leaves.

Supplemental Figure S2. 7,7,8,8-d4-Palmitoyl-ACP specificity of recombinant MS2 and the mass spectra of fatty alcohols.

Supplemental Figure S3. Specificity detection of MS2 antibody.

Supplemental Figure S4. Western-blot analysis of MS2 expressed in tobacco leaves.

Supplemental Table S1. Substrate preference of MS2.

Supplemental Table S2. Detailed wax compositions in transient tobacco leaves.

Supplemental Table S3. Detailed internal lipid compositions in transient tobacco leaves.

Supplemental Table S4. Detailed cutin compositions in transient tobacco leaves.

Supplemental Table S5. List of the primers used for vector construction.

ACKNOWLEDGMENTS

We acknowledge Prof. Hongquan Yang for providing the vector p*A7-YFP*, Prof. George P. Lomonossoff for the vector p*EAQ*, Dr. Hyun-Sook Pai for the marker *F1ATPase-γ-RFP*, and the Arabidopsis Biological Resource Center for the T-DNA insertion line (SAIL_92_C07).

Received June 17, 2011; accepted July 29, 2011; published August 3, 2011.

LITERATURE CITED

Aarts MG, Hodge R, Kalantidis K, Florack D, Wilson ZA, Mulligan BJ, Stiekema WJ, Scott R, Pereira A (1997) The Arabidopsis MALE STERILITY 2 protein shares similarity with reductases in elongation/condensation complexes. Plant J **12:** 615–623

Aarts MG, Keijzer CJ, Stiekema WJ, Pereira A (1995) Molecular characterization of the *CER1* gene of *Arabidopsis* involved in epicuticular wax biosynthesis and pollen fertility. Plant Cell **7:** 2115–2127

Ahlers F, Thom I, Lambert J, Kuckuk R, Rolf W (1999) 1H NMR analysis of sporopollenin from *Typha angustifolia*. Phytochemistry **50:** 1095–1098

Ariizumi T, Hatakeyama K, Hinata K, Inatsugi R, Nishida I, Sato S, Kato T, Tabata S, Toriyama K (2004) Disruption of the novel plant protein NEF1 affects lipid accumulation in the plastids of the tapetum and exine formation of pollen, resulting in male sterility in *Arabidopsis thaliana*. Plant J **39:** 170–181

Ariizumi T, Hatakeyama K, Hinata K, Sato S, Kato T, Tabata S, Toriyama K (2003) A novel male-sterile mutant of *Arabidopsis thaliana*, *faceless pollen-1*, produces pollen with a smooth surface and an acetolysis-sensitive exine. Plant Mol Biol **53:** 107–116

Ariizumi T, Toriyama K (2011) Genetic regulation of sporopollenin synthesis and pollen exine development. Annu Rev Plant Biol **62:** 1.1–1.24

Aya K, Ueguchi-Tanaka M, Kondo M, Hamada K, Yano K, Nishimura M, Matsuoka M (2009) Gibberellin modulates anther development in rice via the transcriptional regulation of GAMYB. Plant Cell **21:** 1453–1472

Bedinger P (1992) The remarkable biology of pollen. Plant Cell **4:** 879–887

Blackmore S, Wortley AH, Skvarla JJ, Rowley JR (2007) Pollen wall development in flowering plants. New Phytol **174:** 483–498

Bonaventure G, Beisson F, Ohlrogge J, Pollard M (2004) Analysis of the aliphatic monomer composition of polyesters associated with Arabidopsis epidermis: occurrence of octadeca-cis-6, cis-9-diene-1,18-dioate as the major component. Plant J **40:** 920–930

Broadwater JA, Fox BG (1999) Spinach holo-acyl carrier protein: overproduction and phosphopantetheinylation in Escherichia coli BL21(DE3), in vitro acylation, and enzymatic desaturation of histidine-tagged isoform I. Protein Expr Purif **15:** 314–326

Brooks J, Shaw G (1968) Chemical structure of the exine of pollen walls and a new function for carotenoids in nature. Nature **219:** 532–533

Bubert H, Lambert J, Steuernagel S, Ahlers F, Wiermann R (2002) Continuous decomposition of sporopollenin from pollen of *Typha angustifolia* L. by acidic methanolysis. Z Naturforsch **57c:** 1035–1071

Cameron KD, Teece MA, Smart LB (2006) Increased accumulation of cuticular wax and expression of lipid transfer protein in response to periodic drying events in leaves of tree tobacco. Plant Physiol **140:** 176–183

Chaloner W (1976) The evolution of adaptive features in fossil exines. *In* IK Ferguson, J Muller, eds, Evolutionary Significance of the Exine. Academic Press, London, pp 1–14

Cheng JB, Russell DW (2004) Mammalian wax biosynthesis. I. Identification of two fatty acyl-coenzyme A reductases with different substrate specificities and tissue distributions. J Biol Chem **279:** 37789–37797

Choi H, Jin JY, Choi S, Hwang JU, Kim YY, Suh MC, Lee Y (2011) An ABCG/WBC-type ABC transporter is essential for transport of sporopollenin precursors for exine formation in developing pollen. Plant J **65:** 181–193

Clement C, Pacini E (2001) Anther plastids in angiosperms. Bot Rev **67:** 54–73

de Azevedo Souza C, Kim SS, Koch S, Kienow L, Schneider K, McKim SM, Haughn GW, Kombrink E, Douglas CJ (2009) A novel fatty acyl-CoA synthetase is required for pollen development and sporopollenin biosynthesis in *Arabidopsis*. Plant Cell **21:** 507–525

Doan TT, Carlsson AS, Hamberg M, Bülow L, Stymne S, Olsson P (2009) Functional expression of five Arabidopsis fatty acyl-CoA reductase genes in *Escherichia coli*. J Plant Physiol **166:** 787–796

Dobritsa AA, Lei ZT, Nishikawa SI, Urbanczyk-Wochniak E, Huhman DV, Preuss D, Sumner LW (2010) LAP5 and LAP6 encode anther-specific proteins with similarity to chalcone synthase essential for pollen exine development in Arabidopsis. Plant Physiol **153:** 937–955

Dobritsa AA, Shrestha J, Morant M, Pinot F, Matsuno M, Swanson R, Møller BL, Preuss D (2009) CYP704B1 is a long-chain fatty acid ω-hydroxylase essential for sporopollenin synthesis in pollen of Arabidopsis. Plant Physiol **151:** 574–589

Domergue F, Vishwanath SJ, Joubès J, Ono J, Lee JA, Bourdon M, Alhattab R, Lowe C, Pascal S, Lessire R, et al (2010) Three Arabidopsis fatty acyl-coenzyme A reductases, FAR1, FAR4, and FAR5, generate primary fatty alcohols associated with suberin deposition. Plant Physiol **153:** 1539–1554

Dou XY, Zhang KZ, Zhang Y, Wang W, Liu XL, Chen LQ, Zhang XQ, Ye D (2011) WBC27, an adenosine tri-phosphate-binding cassette protein, controls pollen wall formation and patterning in Arabidopsis. J Integr Plant Biol **53:** 74–88

Franke R, Briesen I, Wojciechowski T, Faust A, Yephremov A, Nawrath C, Schreiber L (2005) Apoplastic polyesters in *Arabidopsis* surface tissues: a typical suberin and a particular cutin. Phytochemistry **66:** 2643–2658

Grienenberger E, Kim SS, Lallemand B, Geoffroy P, Heintz D, Souza CdeA, Heitz T, Douglas CJ, Legrand M (2010) Analysis of TETRAKETIDE α-PYRONE REDUCTASE function in *Arabidopsis thaliana* reveals a previ-

ously unknown, but conserved, biochemical pathway in sporopollenin monomer biosynthesis. Plant Cell **22:** 4067–4083

He XF, Fang YY, Feng L, Guo HS (2008) Characterization of conserved and novel microRNAs and their targets, including a TuMV-induced TIR-NBS-LRR class R gene-derived novel miRNA in Brassica. FEBS Lett **582:** 2445–2452

Hu LF, Tan HX, Liang WQ, Zhang DB (2010) The *Post-meiotic Deficient Anther1* (*PDA1*) gene is required for post-meiotic anther development in rice. J Genet Genomics **37:** 37–46

Hu SW, Fan YF, Zhao HX, Guo XL, Yu CY, Sun GL, Dong CH, Liu SY, Wang HZ (2006) Analysis of *MS2Bnap* genomic DNA homologous to *MS2* gene from Arabidopsis thaliana in two dominant digenic male sterile accessions of oilseed rape (*Brassica napus* L.). Theor Appl Genet **113:** 397–406

Huang YH, Liang WQ, Pan AH, Zhou ZA, Huang C, Chen JQ, Zhang DB (2003) Production of FaeG, the major subunit of K88 fimbriae, in transgenic tobacco plants and its immunogenicity in mice. Infect Immun **71:** 5436–5439

Huysmans S, El-Ghazaly G, Smets E (1998) Orbicules in angiosperms: morphology, function, distribution, and relation with tapetum types. Bot Rev **64:** 240–272

Jung KH, Han MJ, Lee DY, Lee YS, Schreiber L, Franke R, Faust A, Yephremov A, Saedler H, Kim YW, et al (2006) *Wax-deficient anther1* is involved in cuticle and wax production in rice anther walls and is required for pollen development. Plant Cell **18:** 3015–3032

Kim M, Lim JH, Ahn CS, Park K, Kim GT, Kim WT, Pai HS (2006) Mitochondria-associated hexokinases play a role in the control of programmed cell death in *Nicotiana benthamiana*. Plant Cell **18:** 2341–2355

Kim S, Lee DS, Choi IS, Ahn SJ, Kim YH, Bae HJ (2010a) *Arabidopsis thaliana* Rubisco small subunit transit peptide increases the accumulation of *Thermotoga maritima* endoglucanase Cel5A in chloroplasts of transgenic tobacco plants. Transgenic Res **19:** 489–497

Kim SS, Grienenberger E, Lallemand B, Colpitts CC, Kim SY, Souza CdeA, Geoffroy P, Heintz D, Krahn D, Kaiser M, et al (2010b) LAP6/POLYKETIDE SYNTHASE A and LAP5/POLYKETIDE SYNTHASE B encode hydroxyalkyl α-pyrone synthases required for pollen development and sporopollenin biosynthesis in *Arabidopsis thaliana*. Plant Cell **22:** 4045–4066

Kolattukudy PE (1970) Reduction of fatty acids to alcohols by cell-free preparations of Euglena gracilis. Biochemistry **9:** 1095–1102

Kunst L, Samuels AL (2003) Biosynthesis and secretion of plant cuticular wax. Prog Lipid Res **42:** 51–80

Li H, Pinot F, Sauveplane V, Werck-Reichhart D, Diehl P, Schreiber L, Franke R, Zhang P, Chen L, Gao YW, et al (2010) Cytochrome P450 family member CYP704B2 catalyzes the omega-hydroxylation of fatty acids and is required for anther cutin biosynthesis and pollen exine formation in rice. Plant Cell **22:** 173–190

Li H, Yuan Z, Vizcay-Barrena G, Yang CY, Liang WQ, Zong J, Wilson Z, Zhang DB (2011) *PERSISTENT TAPETAL CELL1* encodes a PHD-finger protein that is required for tapetal cell death and pollen development in rice. Plant Physiol **156:** 615–630

Li H, Zhang DB (2010) Biosynthesis of anther cuticle and pollen exine in rice. Plant Signal Behav **5:** 1121–1123

Li N, Zhang DS, Liu HS, Yin CS, Li XX, Liang WQ, Yuan Z, Xu B, Chu HW, Wang J, et al (2006) The rice *Tapetum Degeneration Retardation* gene is required for tapetum degradation and anther development. Plant Cell **18:** 2999–3014

Li-Beisson YH, Shorrosh B, Beisson F, Andersson MX, Arondel V, Bates PD, Baud S, Bird D, DeBono A, Durrett TP, et al (2010) Acyl-lipid metabolism. The Arabidopsis Book **8:** e0133, doi/10.1199/tab.013

Metz JG, Pollard MR, Anderson L, Hayes TR, Lassner MW (2000) Purification of a jojoba embryo fatty acyl-coenzyme A reductase and expression of its cDNA in high erucic acid rapeseed. Plant Physiol **122:** 635–644

Morant M, Jørgensen K, Schaller H, Pinot F, Møller BL, Werck-Reichhart D, Bak S (2007) CYP703 is an ancient cytochrome P450 in land plants catalyzing in-chain hydroxylation of lauric acid to provide building blocks for sporopollenin synthesis in pollen. Plant Cell **19:** 1473–1487

Moto K, Yoshiga T, Yamamoto M, Takahashi S, Okano K, Ando T, Nakata T, Matsumoto S (2003) Pheromone gland-specific fatty-acyl reductase of the silkmoth, *Bombyx mori*. Proc Natl Acad Sci USA **100:** 9156–9161

Ohlrogge JB, Kuhn DN, Stumpf PK (1979) Subcellular localization of acyl carrier protein in leaf protoplasts of *Spinacia oleracea*. Proc Natl Acad Sci USA **76:** 1194–1198

Paxson-Sowders DM, Dodrill CH, Owen HA, Makaroff CA (2001) DEX1, a novel plant protein, is required for exine pattern formation during pollen development in Arabidopsis. Plant Physiol **127:** 1739–1749

Piffanelli P, Ross JH, Murphy DJ (1998) Biogenesis and function of the lipidic structures of pollen grains. Sex Plant Reprod **11:** 65–80

Pollard M, Beisson F, Li Y, Ohlrogge JB (2008) Building lipid barriers: biosynthesis of cutin and suberin. Trends Plant Sci **13:** 236–246

Quilichini TD, Friedmann MC, Samuels AL, Douglas CJ (2010) ATP-binding cassette transporter G26 is required for male fertility and pollen exine formation in Arabidopsis. Plant Physiol **154:** 678–690

Ritter K (1991) Affinity purification of antibodies from sera using polyvinylidenedifluoride (PVDF) membranes as coupling matrices for antigens presented by autoantibodies to triosephosphate isomerase. J Immunol Methods **137:** 209–215

Rock CO, Garwin JL (1979) Preparative enzymatic synthesis and hydrophobic chromatography of acyl-acyl carrier protein. J Biol Chem **254:** 7123–7128

Rowland O, Zheng H, Hepworth SR, Lam P, Jetter R, Kunst L (2006) *CER4* encodes an alcohol-forming fatty acyl-coenzyme A reductase involved in cuticular wax production in Arabidopsis. Plant Physiol **142:** 866–877

Sainsbury F, Lomonossoff GP (2008) Extremely high-level and rapid transient protein production in plants without the use of viral replication. Plant Physiol **148:** 1212–1218

Shi J, Tan HX, Yu XH, Liu YY, Liang WQ, Ranathunge K, Franke RB, Schreiber L, Wang YJ, Kai GY, et al (2011) *Defective Pollen Wall* is required for anther and microspore development in rice and encodes a fatty acyl carrier protein reductase. Plant Cell **23:** 2225–2246

Tang LK, Chu H, Yip WK, Yeung EC, Lo C (2009) An anther-specific dihydroflavonol 4-reductase-like gene (DRL1) is essential for male fertility in Arabidopsis. New Phytol **181:** 576–587

Wang A, Xia Q, Xie W, Dumonceaux T, Zou J, Datla R, Selvaraj G (2002) Male gametophyte development in bread wheat (*Triticum aestivum* L.): molecular, cellular, and biochemical analyses of a sporophytic contribution to pollen wall ontogeny. Plant J **30:** 613–623

Wilson ZA, Morroll SM, Dawson J, Swarup R, Tighe PJ (2001) The *Arabidopsis MALE STERILITY1* (*MS1*) gene is a transcriptional regulator of male gametogenesis, with homology to the PHD-finger family of transcription factors. Plant J **28:** 27–39

Xu J, Yang C, Yuan Z, Zhang D, Gondwe MY, Ding Z, Liang W, Zhang D, Wilson ZA (2010) The ABORTED MICROSPORES regulatory network is required for postmeiotic male reproductive development in *Arabidopsis thaliana*. Plant Cell **22:** 91–107

Yi B, Zeng FQ, Lei S, Chen Y, Yao X, Zhu Y, Wen J, Shen J, Ma C, Tu J, et al (2010) Two duplicate *CYP704B1*-homologous genes *BnMs1* and *BnMs2* are required for pollen exine formation and tapetal development in *Brassica napus*. Plant J **63:** 925–938

Yoo SD, Cho YH, Sheen J (2007) Arabidopsis mesophyll protoplasts: a versatile cell system for transient gene expression analysis. Nat Protoc **2:** 1565–1572

Zhang DS, Liang W, Yin C, Zong J, Gu F, Zhang D (2010) OsC6, encoding a lipid transfer protein, is required for postmeiotic anther development in rice. Plant Physiol **154:** 149–162

Zhang DS, Liang WQ, Yuan Z, Li N, Shi J, Wang J, Liu YM, Yu WJ, Zhang DB (2008) *Tapetum degeneration retardation* is critical for aliphatic metabolism and gene regulation during rice pollen development. Mol Plant **1:** 599–610

Zhang D, Luo X, Zhu L (August 10, 2011) Cytological analysis and genetic control of rice anther development. J Genet Genomics http://dx.doi.org/10.1016/j.jgg.2011.08.001

Zinkl GM, Zwiebel BI, Grier DG, Preuss D (1999) Pollen-stigma adhesion in *Arabidopsis*: a species-specific interaction mediated by lipophilic molecules in the pollen exine. Development **126:** 5431–5440